Supplemental Materials

Supplemental Text

C. elegans, like all organisms, must effectively manage energy reserves throughout their life in order to optimize survival and reproduction[1]. The regulation of fat homeostasis integrates genetic pathways that function in nutrient uptake, storage, and utilization, which have obvious influences on metabolism but can also impact reproduction and lifespan[2-8]. The sensing of available nutrients and the metabolic state of the organism can potently influence these physiological pathways. Previous studies have focused on the developmental programs that underlie fat storage capacity[9]; leaving a gap in our understanding of how lipid homeostasis is maintained in later adult stages. In particular, the regulatory mechanisms that balance resources between somatic (survival-promoting) and germ (reproduction-promoting) cells and the resulting physiological consequence of aberrant reallocation within intact animals (functional soma and germline) are largely unknown.

Asdf is a diet-dependent phenotype

Many metabolic phenotypes are not only sensitive to the amount of food ingested but also integrate information regarding the composition of the diet[5,10-12]. Similar to wild type animals feeding of an HT115/ *E. coli* K-12 bacterial diet increased early reproductive output of the SKN-1gf mutant animals (Fig. S7a and Table S2), but also abolished the extended self-reproduction (Fig. S7b-n and Table S2) period of the SKN-1gf mutants and suppressed the Asdf phenotype (Fig. S7b-n). As such, we adopted an OP50/*E.coli* B strain capable of generating dsRNA for all of our feeding RNAi experiments (Table S3).

We developed a strategy to assess the temporal requirement of the OP50 diet to induce Asdf at 144-hours post feeding (Fig. S7o). The suppression of Asdf was fully penetrant when animals were switched from the OP50 to HT115 diet just prior to adulthood (48-hours post feeding) (Fig. S7p), but the influence of diet was less pronounced - i.e. a small percentage of animals still display Asdf - when the switch to the HT115 diet was done in reproductively active animals (96-hours post feeding) (Fig. S7q), consistent with the prediction that Asdf is important later in reproduction. One major difference in the macronutrient complexity of the HT115 diet is the

high carbohydrate composition as compared to OP50[13]. Intriguingly, supplementation of the OP50 diet with 2% glucose was also capable of suppressing Asdf in the SKN-1gf mutants (Fig. S7r-u), indicating the soma-to-germline mobilization of lipids is sensitive to the abundance of dietary carbohydrates.

The importance of characterizing the specific composition of the diet utilized in physiological measurements is becoming increasingly appreciated[5,10-12]; especially in the context of SKN-1 dependent phenotypes. The proper identification of *skn-1* and the vitellogenin family of genes in the regulation of Asdf required the development of an OP50 (*E. coli* B*)* derived RNAi competent strain, as the high carbohydrate composition of the HT115 diet could potently suppress Asdf. In addition to glucose, we identified an important role for oleic acid in the propensity for animals to display Asdf. Oleic acid levels are directly tied to the availability of carbohydrates in the diet [14]. Importantly, suppression of Asdf by fatty acid supplementation is specific to oleic acid and is not simply a result of making animals fatter. These findings further emphasize the importance of considering the impact that diet will have on the experimental output of all studies and will be of importance to laboratory-based studies and ecological studies examining wild animals and their dietary history.

Materials and Methods:

C. elegans and *E. coli* strains and culture conditions

C. elegans were cultured using standard techniques at 20°C [15] unless otherwise noted. The following strains were used: wild-type N2 Bristol, SPC207: *skn-1(lax120)*, SPC227: *skn-1(lax188)*, SPC321: *alh-6(lax105)*, SPC303: *wdr-23 (lax211)*, VC1772 (*skn-1(ok2315) IV/nT1[qIs51](IV;V)),* BX52: *fat-4(wa14);fat-1(wa9)*, DA453: *eat-2(ad456)*, MQ887: *isp-1(qm150)*, DR1572: *daf-2(e1368)*; natural isolates: NL7000, ED3040, ED3021, TR403, CB4856, CB4869, RW7000, ED3049. Staged animals were obtained by washing animals each day to new plates during the reproductive period, allowing adults to settle by gravity, dropping samples on plates, and burning off any progeny missed in the wash steps.

E.coli strains were grown in LB supplemented with appropriate antibiotic(s) for selection. The following strains were used: OP50 – *E.coli* B, ura, OP50-RNAi (described below) *E.coli* B, rnc14::ΔTn10, laczγA::T7pol, HT115(DE3) - Derived from *E. coli* K12, F-, mcrA, mcrB, IN(rrnD-rrnE)1, rnc14::Tn10 (DE3 lysogen: lacUV5 promoter –T7 polymerase). All experiments used plates with freshly seeded *E.coli,* from cultures grown for 16-18 hours (h) "overnight" (O/N) at 37°C, and inoculated from stock plates less than 1-month of age.

GC-MS

Samples were grown in triplicate on OP50 with and without 2% glucose supplementation (see below). At larval-stage 4 (L4), 7500 animals were washed three times with 1X PBS, then pelleted at 20,000 x *g* and supernatant was aspirated off. Afterwards, samples were promptly frozen at -80°C. Lipid extracts from these samples were analyzed by solid-phase chromatography followed by GCMS as previously reported [5,16]. For all measurements, at least two biological replicates were performed, with data shown as mean ± SEM.

Lipid staining

Oil-red-O (ORO) or fixed Nile red staining [4] was conducted by washing 200-300 animals from experimental plates synchronized by egg-prep with 1x PBS + 0.01% Triton X-100 (PBST). Worms were washed three times with 1x PBST and allowed to settle by gravity. To permeabilize the cuticle, worms were resuspended in 100µl 1x PBST and 600µl of 40% isopropanol was added while samples were rocked for three minutes. Worms were spun down at 500 RPM for 30s and 600µl was aspirated off. Then, 600µl of 60% ORO working stock solution is added and samples are rotated at room temperature (RT) – 21.0-23.5°C for two hours. ORO working stock was prepared as follows: a 0.5g of ORO in 100mL isopropanol is stirred O/N and on the day of staining, is freshly diluted to 60% with water and rocked for two hours, and debris removed through a 0.22µm-filter. Worm samples are pelleted at 500 RPM for 30s, 600µl of solution is aspirated off, and 600µl of PBST is added. Samples are rotated for another 30 minutes at RT and then animals were mounted on slides in the presence of DAPI (internal control for permeabilization of animals) and imaged with a color camera (Zeiss AxioCam ERc5s) outfitted with DIC optics. A minimum of twenty animals were imaged in a minimum of two independent biological replicates and results were consistent between biological replicates.

Assessment of Asdf capacity

ORO stained samples were processed as indicated above and images collected. Percent (%) Asdf is quantified by counting the number of animals in a cohort that display the phenotype compared to the number of animals that do not. A minimum of two independent experiments

with 2-3 biological replicates, n=4 to 6 are performed. Although hundreds of animals are examined and scored over all replicates, the calculated % Asdf presented in each figure and Supplemental Fig. 3 only accounts for whole and non-overlapping animals in the field of view and where the germline and soma are clearly defined. Blind scoring of % Asdf in each sample is then independently assessed by two individuals and their results compiled to reflect %Asdf of the population.

Reproduction assays

L1 stage animals were synchronized by egg prep, rocked O/N at 20°C, and dropped onto experimental plates the next morning. 48-hours post-feeding, ten L4 stage animals of each strain and diet were moved to their own respective experimental plate. These animals were then assigned a number and their reproductive output was tracked, twice daily, by moving each animal to a fresh plate every twelve hours until reproduction ceased. To ensure accurate counts of progeny number, each plate was assessed at least twice; 24 to 48-h after the hermaphrodite mother was moved from the plate.

RNAi OP50 strain construction

RNAi OP50 was created by replacing the WT OP50 allele of RNAIII RNase (rnc) with a deletion allele and introducing an IPTG-inducible T7 RNA polymerase. P1 phage lysates were prepared from strains HT115 (rnc14::ΔTn10) and CH1681(laczγA::T7pol camFRT). To generate the OP50 (rnc14::ΔTn10) strain, an overnight culture of OP50 was transduced with an equal volume of HT115 P1 lysate and plated on LB+tet+citrate plates. Positive colonies were re-selected three times on LB+tet+citrate media plates. Individual colonies were subsequently inoculated into LB+tet and the presence of rnc14::ΔTn10 allele was confirmed by PCR. To generate the RNAi-competent OP50 strain an overnight culture of OP50 (rnc14::ΔTn10) was transduced with equal volume of Ch1681 P1 lysate and selected on LB+cam+citrate plates. Positive colonies were restreaked three times onto LB+cam+citrate media plates. Individual colonies, were subsequently inoculated into LB+tet+cam and the presence of rnc14::ΔTn10 and laczγA::T7pol was confirmed by PCR.

RNA interference (RNAi)

An RNAse III-deficient OP50 *E. coli* B strain was engineered for IPTG-inducible expression of T7 polymerase (See above). Sequence verified double stranded RNA-expression plasmids were transformed into this strain. RNAi feeding plates were prepared using standard NGM recipe with 5mM isopropyl-β-D-thiogalactoside (IPTG) and 50 ug/ml carbenicillin. Synchronized L1 animals were added to plates to knockdown indicated genes.

Lipid feeding (supplementation assays)

Fatty acid supplementation plates were made using an adapted protocol [17]. In brief, 100mM aqueous solution stocks of each supplement were first made. These were made fresh right before pouring regular NGM plates containing 0.1% tergitol (NP40) and added to NGM media once cooled to 55°C at the concentrations indicated. Oleic acid (#90260), Stearic acid (#10011298), Lauric acid (#10006626), Linoleic acid (#90150), a-linolenic acid (#90210), g-linolenic acid (#90220), *trans*-vaccenic acid (#15301), and DGLA (#90230) were purchased from Cayman Chemical and AA (#A9673) and EPA (#E2011) were purchased from Sigma Aldrich.

Glucose supplementation

Glucose was added to NGM media, cooled to 55°C, to obtain a final concentration of 2% glucose in the worm plates.

Starvation and matricide assays
Staged adult animals were washed 5 times in 1x PBS to get rid of any food, transferred to 15mL conical tubes, and 10mL of liquid NGM (prepared just like NGM media but without agar) was added to ~50ul of washed worms. Volumes of liquid NGM were adjusted accordingly to make maintain worm density across experiments. Tubes were gently rotated overnight at 20°C and 24 hours later, total lipid (ORO) and the frequency of the Bag phenotype (more than one internally hatched progeny) was assessed by microscopy.

Oxidative stress assays
Staged animals were collected and washed with 1x Phosphate Buffered Saline + Triton X-100 (PBST) three times to remove any contamination from the bacterial food source. After the final wash, the animals were allowed to settle, by gravity, and the supernatant was aspirated leaving ~100ul behind. 1mL of H2O2 solution (concentrations ranging between 2mM to 10mM) in 1x PBST was added to each experimental tube of worms. Tubes were gently rotated at RT for 20 minutes, followed by centrifugation at 500 RPM for 30s and the worms were washed three times in 1X PBST. After the final wash animals were dropped onto seeded NGM plates for recovery. Recovery times (as indicated) varied between 12 and 24 hours before analysis. ORO staining and imaging was used for fat depletion analysis while survival was recorded based on head response from prodding with a platinum wire.

NAC assays
N-acetyl-cysteine (NAC) solution in water was added to the top of a seeded worm plate at a final concentration of 10mM and allowed to dry in a sterile hood. The solution was made to cover the entirety of the 300ul bacterial lawn. Synchronized animals were moved to these plates at the L1 stage, kept on this diet their whole lives, and then total lipids stained and imaged at the specified times.

Heat shock assay
Synchronized L1 wild type animals were raised on normal OP50 bacteria seeded worm plates for 72 hours at 20°C. Then, plates were transferred to 30°C for 9 hours. After that time, plates were transferred back to 20°C and worms were allowed to recover O/N. At 96-hours post feeding, total lipids were stained and imaged. Adapted from Walker et al.[18].

Osmotic stress assay
NGM plates were prepared with 11.67g/L of NaCl (instead of 3.0g/L, as normal) for 200mM final concentration and were subsequently seeded with OP50 bacteria. Synchronized wild type animals were moved to these plates at the L1 stage, kept on these plates their whole lives, and then total lipids stained and imaged at 144-hours post feeding. Adapted from Lamitina et al.[19].

Statistics
Statistical analyses were performed with GraphPad Prism 6 software. Data are presented as mean±s.e.m. Data were analyzed by using unpaired Student's t-test and two-way ANOVA. $P<0.05$ was considered as significant.

References

1 Ashrafi, K. Obesity and the regulation of fat metabolism. *WormBook*, 1-20, doi:10.1895/wormbook.1.130.1 (2007).

2 Curran, S. & Ruvkun, G. Lifespan regulation by evolutionarily conserved genes essential for viability. *PLoS Genet* **3**, e56, doi:10.1371/journal.pgen.0030056 (2007).

3 Tacutu, R. *et al.* Prediction of C. elegans Longevity Genes by Human and Worm Longevity Networks. *PLoS One* **7**, e48282, doi:10.1371/journal.pone.0048282 (2012).

4 O'Rourke, E. J., Soukas, A. A., Carr, C. E. & Ruvkun, G. C. elegans major fats are stored in vesicles distinct from lysosome-related organelles. *Cell Metab* **10**, 430-435, doi:10.1016/j.cmet.2009.10.002 (2009).

5 Soukas, A. A., Kane, E. A., Carr, C. E., Melo, J. A. & Ruvkun, G. Rictor/TORC2 regulates fat metabolism, feeding, growth, and life span in Caenorhabditis elegans. *Genes & development* **23**, 496-511, doi:10.1101/gad.1775409 (2009).

6 Hansen, M., Flatt, T. & Aguilaniu, H. Reproduction, fat metabolism, and life span: what is the connection? *Cell Metab* **17**, 10-19, doi:10.1016/j.cmet.2012.12.003 (2013).

7 Khanna, A., Johnson, D. L. & Curran, S. P. Physiological roles for mafr-1 in reproduction and lipid homeostasis. *Cell reports* **9**, 2180-2191, doi:10.1016/j.celrep.2014.11.035 (2014).

8 Vrablik, T. L. & Watts, J. L. Polyunsaturated fatty acid derived signaling in reproduction and development: insights from Caenorhabditis elegans and Drosophila melanogaster. *Molecular reproduction and development* **80**, 244-259, doi:10.1002/mrd.22167 (2013).

9 Mak, H. Y. Lipid droplets as fat storage organelles in Caenorhabditis elegans: Thematic Review Series: Lipid Droplet Synthesis and Metabolism: from Yeast to Man. *J Lipid Res* **53**, 28-33, doi:10.1194/jlr.R021006 (2012).

10 Maier, W., Adilov, B., Regenass, M. & Alcedo, J. A neuromedin U receptor acts with the sensory system to modulate food type-dependent effects on C. elegans lifespan. *PLoS Biol* **8**, e1000376, doi:10.1371/journal.pbio.1000376 [doi] (2010).

11 Pang, S. & Curran, S. P. Adaptive Capacity to Bacterial Diet Modulates Aging in C. elegans. *Cell Metab* **19**, 221-231, doi:10.1016/j.cmet.2013.12.005 (2014).

12 Pang, S., Lynn, D. A., Lo, J. Y., Paek, J. & Curran, S. P. SKN-1 and Nrf2 couples proline catabolism with lipid metabolism during nutrient deprivation. *Nature communications* **5**, 5048, doi:10.1038/ncomms6048 (2014).

13 Brooks, K. K., Liang, B. & Watts, J. L. The influence of bacterial diet on fat storage in C. elegans. *PLoS One* **4**, e7545, doi:10.1371/journal.pone.0007545 (2009).

14 Merkel, M., Velez-Carrasco, W., Hudgins, L. C. & Breslow, J. L. Compared with saturated fatty acids, dietary monounsaturated fatty acids and carbohydrates increase atherosclerosis and VLDL cholesterol levels in LDL receptor-deficient, but not apolipoprotein E-deficient, mice. *Proc Natl Acad Sci U S A* **98**, 13294-13299, doi:10.1073/pnas.231490498 (2001).

15 Brenner, S. The genetics of Caenorhabditis elegans. *Genetics* **77**, 71-94 (1974).

16 Perez, C. L. & Van Gilst, M. R. A 13C isotope labeling strategy reveals the influence of insulin signaling on lipogenesis in C. elegans. *Cell Metab* **8**, 266-274, doi:10.1016/j.cmet.2008.08.007 (2008).

17 Deline, M. L., Vrablik, T. L. & Watts, J. L. Dietary supplementation of polyunsaturated fatty acids in Caenorhabditis elegans. *J Vis Exp*, doi:10.3791/50879 (2013).

18 Walker, G. A. *et al.* Heat shock protein accumulation is upregulated in a long-lived mutant of Caenorhabditis elegans. *J Gerontol A Biol Sci Med Sci* **56**, B281-287 (2001).
19 Lamitina, T., Huang, C. G. & Strange, K. Genome-wide RNAi screening identifies protein damage as a regulator of osmoprotective gene expression. *Proc Natl Acad Sci U S A* **103**, 12173-12178, doi:10.1073/pnas.0602987103 (2006).

Supplemental Figure Legends

Figure S1. ORO Asdf progression in wild type and SKN-1(gf) mutants.
(a) Daily progeny production of OP50-fed wild type (blue circle) and SKN-1gf mutant (red square) animals, $*P < 0.05$, $**P < 0.01$, two-tailed *t* test. Oil-red-O staining of total lipids in (b-e) Wild type, (f-i) SKN-1gf*(lax188)*, and (j-m) SKN-1gf*(lax120)* adult animals during reproduction.

Figure S2. NR Asdf progression in wild type and SKN-1(gf) mutants.
Nile red staining of total lipids in (a-d) Wild type, (e-h) SKN-1gf*(lax188)*, and (i-l) SKN-1gf*(lax120)* adult animals during reproduction. Where labeled, arrows point to somatic lipids and arrowheads denote germline lipids in oocytes

Figure S3. Cohort analysis of %Asdf.
% Asdf is quantified by counting the number of animals in a cohort that display the phenotype compared to the number of animals that do not. Mean ± SEM, *n* = # of animals used from at two of the biological replicates performed to calculate % Asdf.

Figure S4. SKN-1 activation and oxidative stress induce Asdf.
(a-f) SKN-1 activation is sufficient to induce Asdf as observed in (a-b) *alh-6(lax105),* (c-d) *wdr-23(lax211)*, and (e-f) acute exposure to hydrogen peroxide (H2O2), but not (g) heat shock or (h) osmotic stress but is dependent on (i-j) *skn-1*. (k-p) Dietary supplementation of the antioxidant N-acetylcysteine (NAC) suppresses Asdf in (k-l) *alh-6(lax105)* and (m-n) *skn-1(lax188)gf* and increases somatic fat in (o-p) wild type. (q-r) *skn-1* RNAi and (s-t) *skn*-1 null mutants display increased somatic fat as compared to controls.

Figure S5. Vitellogenin proteins transport lipids from the soma to the germline in animals with Asdf.
(a-d) Fixed Nile red staining of total lipids in animals treated with RNAi of the vitellogenin family of proteins: (a) control RNAi, (b) *vit-3* RNAi, (c) *vit-4* RNAi, (d) *vit-5* RNAi; suppresses the somatic transfer of lipids to the germline in SKN-1gf animals with Asdf.

Figure S6. Asdf is a specific response to nutrient deprivation.
(a-f) Fixed Nile red staining of mutant animals. (a-b) WT, (c-d) *eat-2* mutants in early reproduction do not display Asdf while *eat-2* mutants late in reproduction do display Asdf (d). Long-lived (e-f) *daf-2*(insulin receptor) do not display Asdf. (g-j) Oil red O staining reveals lack of Asdf in (g-h) wild type and (i-j) *isp-1*(mitochondrial iron sulfur cluster protein) mutants. Notes: exposure time for *daf-2* mutants with fixed Nile red fluorescence was 50% of WT as to properly resolve structures. *daf-2* mutant animals were grown at 20C until L2/L3 stage and then moved to 25C, as such 144-h *daf-2* animals are likely developmentally more mature than age-matched controls.

Figure S7. Asdf is a diet-dependent phenotype.
(a) An HT115-diet (green square) increases early daily progeny production and suppresses extended self-reproduction observed in SKN-1gf fed an OP50-diet (red square), $**P < 0.01$, $****P < 0.0001$, two-tailed *t* test. (b) The HT115 bacterial diet suppresses Asdf in SKN-1gf

mutant animals at 144-hours post feeding. Oil-red-O staining of total lipids reveals that Asdf does not occur at any time in reproductive life when an HT115-diet is fed to: Wild type (c-f), SKN-1gf*(lax188)* (g-j), or (k-n) SKN-1gf*(lax120)* adult animals. (o) cartoon representation of diet switching experiments. -, not observed; +, 25-50% of population display Asdf, ++, 50-75% of population display Asdf; +++, 75-100% of population display Asdf. (p) Asdf is fully suppressed in OP50-fed SKN-1gf mutants if switched to an HT115 diet at 48-hours post feeding and (q) partially suppressed when switched at 96-hours post feeding. (r) Glucose supplementation of the OP50 bacterial diet suppresses Asdf in SKN-1gf animals. (s-t) 2% Glucose supplementation of the OP50-diet increases somatic lipid stores in WT animals. (u) *skn-1(lax188)gf* mutants accumulate less somatic lipids on a 2% carbohydrate supplemented OP50-diet early in reproduction. Bar graphs accompanying each panel indicate the percent of population scored with the Asdf phenotype (red) versus normal lipid distribution (black) from a minimum of two biological replicates for each genotype and condition (see Fig. S3 for more detail). Scale bars = 100um.

Figure S8. Oleic acid deficiency in SKN-1gf mutants is reversed by dietary glucose.
(a) GCMS analysis of total fatty acids in the triglyceride fraction of wild type (blue) and SKN-1gf (red) animals fed an OP50-diet, ****$P < 0.0001$, two-tailed *t* test. (b) GCMS analysis of total fatty acids in the triglyceride fraction of wild type (blue) and *skn-1(lax120)gf* (orange) animals fed an OP50-diet. (c) GCMS analysis of total fatty acids in the triglyceride fraction of: WT fed OP50 (dark blue); WT fed OP50+glucose (light blue), *skn-1(lax188)gf* fed OP50 (red), *skn-1(lax188)gf* fed OP50+glucose (purple), *skn-1(lax120)gf* fed OP50 (orange) and *skn-1(lax120)gf* fed OP50+glucose (yellow) animals. (d) Schematic of oleic acid biosynthetic pathway in *C. elegans*. Abbreviations: cyclo, cyclopropane fatty acid; iso, iso-methyl branched chain fatty acid.

Figure S9. Oleic acid deficiency is sufficient to induce Asdf.
(a) Schematic of lipid biosynthesis pathway in *C. elegans.* (b-g) Oleic acid supplementation increases somatic lipids in wild-type and suppresses Asdf in SKN-1gf mutants in a dose dependent manner. Supplementation of stearic acid, lauric acid, linoleic aicd, α-linolenic acid, γ-linolenic acid, or trans-vaccenic acid increases somatic lipids in wild-type (h,i,k,m,o,q) and but does not suppress Asdf in SKN-1gf mutants (j,l,n,p) ****, $P<0.0001$

Figure S10. AA and EPA precursors of eicosanoid signaling molecules influence Asdf.
(a) Eicosanoid-deficient *fat-4(wa14); fat-1(wa9)* mutant animals do not display Asdf early in reproduction (72-hpf). (b-e) Arachadonic acid (ARA) supplementation increases somatic lipids in WT and suppressed Asdf in SKN-1gf mutants. (f-g) Eicosapentaenoic acid (EPA) supplementation increases somatic lipids in WT and suppressed Asdf in SKN-1gf mutants. (h) dihomo-γ-linolenic acid (DGLA) and (i) Eicosatetraenoic acid (ETA) increases somatic lipids in WT as compared to controls (j).

Figure S11. Variation of Asdf among natural isolates of *C. elegans*. Oil-red-O staining of somatic and germline lipids reveals Asdf-capacity (a-d) and -deficiency (e-h) among isolated natural isolates of *C. elegans* at 144-hours post feeding. (i) Daily progeny output of NL7000 (blue circles) and RW7000 (red squares) isolates of *C. elegans Bergerac* strains, *$P < 0.05$, **$P < 0.01$, two-tailed *t* test.. Bar graphs accompanying each panel indicate the percent of

population scored with the Asdf phenotype (red) versus normal lipid distribution (black) from a minimum of two biological replicates for each genotype and condition (see Fig. S3 for more detail). Scale bars = 100um.

Figure S12. Matricide is enhanced in animals with Asdf after 24-hours of starvation.
WT animals in early (a) and late (b) reproductive life do not Bag (> 1 internally hatched worm) after 24-hours of starvation. (c) SKN-1gf mutants, early in reproductive life do not Bag when starved for 24-hours. (d) SKN-1gf mutants, with Asdf, late in reproductive life display a high incidence of matricide when starved for 24-hours. Arrows denote internally hatched larvae.

Figure S13. Survival of acute exposure to hydrogen peroxide is influenced by Asdf.
(a) WT animals early in reproduction are sensitive to acute exposure to H2O2 and more resistant at the end of the reproductive period. (b) SKN-1gf mutant animals are resistant to acute exposure to H2O2 and that resistance declines later in reproduction, which correlates with Asdf. (c) Supplementation of stearic acid or DGLA does not increase somatic resistance to H2O2 early or late in reproduction in SKN-1gf mutants. (d) NL7000 and RW7000 *Bergerac* strains are resistant to H2O2 oxidative stress early in reproduction. ****, $P<0.0001$ two-tailed *t* test.

Table S1. **Daily progeny production for wild type and SKN-1gf on the OP50 diet**

	Hours post feeding (hpf)										
	60	**72**	**84**	**96**	**108**	**120**	**132**	**144**	**156**	**168**	**TOTAL**
WT-1	8	25	50	48	31	Censor[1]					162
WT-2	28	21	38	37	45	Censor[1]					169
WT-3	10	26	36	67	58	13	0	1	0	1	212
WT-4	0	26	42	39	72	49	39	6	0	0	273
WT-5	11	43	68	66	77	8	2	0	1	0	276
WT-6	9	17	37	46	53	29	0	0	2	1	194
WT-7	18	41	48	37	65	35	14	15	9	7	289
WT-8	3	51	69	81	59	5	1	0	0	0	269
WT-9	0	22	56	64	75	70	4	2	0	0	293
WT-10	0	31	63	90	95	40	14	1	2	1	337
Average	**8.7**	**30.3**	**50.7**	**57.5**	**63**	**24.9**	**7.4**	**2.5**	**1.4**	**1**	**267.9**
SKN-1gf-1	0	33	35	55	32	23	14	6	0	6	204
SKN-1gf-2	0	22	39	37	60	16	4	2	1	2	183
SKN-1gf-3	0	22	44	55	70	42	20	16	23	12	304
SKN-1gf-4	3	43	58	63	68	18	13	1	0	1	268
SKN-1gf-5	0	47	54	60	63	40	16	13	9	13	315
SKN-1gf-6	0	18	41	48	49	55	35	21	13	22	302
SKN-1gf-7	0	29	45	25	51	16	14	4	0	7	191
SKN-1gf-8	4	34	47	31	57	43	22	3	3	0	244
SKN-1gf-9	0	18	34	53	19	38	30	22	8	20	242
SKN-1gf-10	0	21	40	52	50	27	19	19	6	13	247
Average	**0.7**	**28.7**	**43.7**	**47.9**	**51.9**	**31.8**	**18.7**	**10.7**	**6.3**	**9.6**	**250**

1. Animals displaying Bag and Pvl phenotypes or escaped the plate were censored.

Table S2. Daily progeny production for wild type and SKN-1gf on the HT115 diet

	Hours post feeding (hpf)										
	60	**72**	**84**	**96**	**108**	**120**	**132**	**144**	**156**	**168**	**TOTAL**
WT-1	72	121	94	34	11	0	1	0	0	0	333
WT-2	60	119	130	55	1	0	0	0	0	0	365
WT-3	86	107	123	72	4	2	0	0	0	0	394
WT-4	75	114	119	48	4	0	0	0	0	0	360
WT-5	77	121	Censored[1]								258
WT-6	80	105	98	47	1	0	0	0	0	0	331
WT-7	73	115	79	22	3	0	0	0	0	0	292
WT-8	59	Censored[1]									115
WT-9	90	127	81	6	0	0	0	0	0	0	304
WT-10	77	112	67	14	11	2	0	0	0	0	283
Average	**74.9**	**109.7**	**85**	**29.8**	**3.6**	**0.4**	**0.1**	**0**	**0**	**0**	**332.8**
SKN-1gf-1	47	82	72	36	1	5	1	0	0	0	244
SKN-1gf-2	64	105	108	41	4	0	0	0	0	0	322
SKN-1gf-3	47	112	116	58	17	0	0	0	0	0	350
SKN-1gf-4	58	102	97	33	0	0	0	0	0	0	290
SKN-1gf-5	63	85	87	17	3	2	0	0	0	0	257
SKN-1gf-6	49	66	Censored[1]								188
SKN-1gf-7	50	100	105	54	7	0	0	0	0	0	316
SKN-1gf-8	64	96	90	45	7	0	0	0	0	0	302
SKN-1gf-9	59	105	104	52	7	0	0	0	0	0	327
SKN-1gf-10	51	124	108	39	0	0	0	0	0	0	322
Average	**55.2**	**97.7**	**94.6**	**38.8**	**4.7**	**0.7**	**0.1**	**0**	**0**	**0**	**291.8**

1. Animals displaying Bag and Pvl phenotypes or escaped the plate were censored.

Table S3. **OP50 RNAi knockdown efficiencies**

Gene	Description[1]	Expression	Significance[3]
skn-1	bZip transcription factor orthologous to the mammalian Nrf (Nuclear factor-erythroid-related factor)	0.609	*
gst-4	SKN-1 target used as second assessment of *skn-1* RNAi efficacy	0.100	***
fat-6	delta-9 fatty acid desaturase	0.068	***
fat-7	delta-9 fatty acid desaturase	0.084	***
vit-2	vitellogenin homolog YP170	0.344	**

1. Gene descriptions provided by WormBase version: WS249

2. mRNA expression levels in SKN-1gf animals treated with indicated RNAi relative to SKN-1gf animals treated with vector control RNAi; normalized to *snb-1* expression as a control, which was invariant across samples. Green and red color indicates increased and decreased expression, respectively.

3. *, *P*-value<0.05; **, *P*-value<0.01; ****, *P*-value<0.0001; n.s., difference between samples in non significant = *P*-value>0.05

Table S4. **mRNA expression levels of oleic acid and eicosanoid biosynthesis pathway genes**

Target	Description[1]	Fold-change[2]	Significance[3]
gst-4	Control for SKN-1 activation	36.76	****
fat-1	omega-3 fatty acyl desaturase	-1.31	*
fat-4	delta-5 fatty acid desaturase	-1.35	n.s.
fat-6	delta-9 fatty acid desaturase	-1.21	n.s.
fat-7	delta-9 fatty acid desaturase	-1.91	*P*=0.05

1. Gene descriptions provided by WormBase version: WS249

2. Fold-change in expression in SKN-1gf mutant animals relative to wild-type animals normalized to *snb-1* expression as a control, which was invariant across samples. Green and red color indicates increased and decreased expression, respectively.

3. *, *P*-value<0.05; **, *P*-value<0.01; ****, *P*-value<0.0001; n.s., difference between samples in non significant = *P*-value>0.05

Table S5. Variation of Asdf phenotype among natural isolates of *C. elegans*.

Strain[1]	Location isolated[2]	Asdf[3]
NL7000	Bergerac, France	+++
ED3040	Johannesburg, South Africa	+++
ED3021	Edinburgh, Scotland	++
ED3049	Ceres, South Africa	+
RW7000	Bergerac, France	-
TR403	Wisconsin, USA	-
CB4869	Vancouver, Canada	-
CB4856	Hawaii, USA	-

1. Strain designation as reported to the *Caenorhabditis* Genetics Center (CGC)
2. Geographic location where strain was isolated (Wormbase)
3. Penetrance of Asdf phenotype. -, not observed; +, 25-50% of population display Asdf, ++, 50-75% of population display Asdf; +++, 75-100% of population display Asdf.

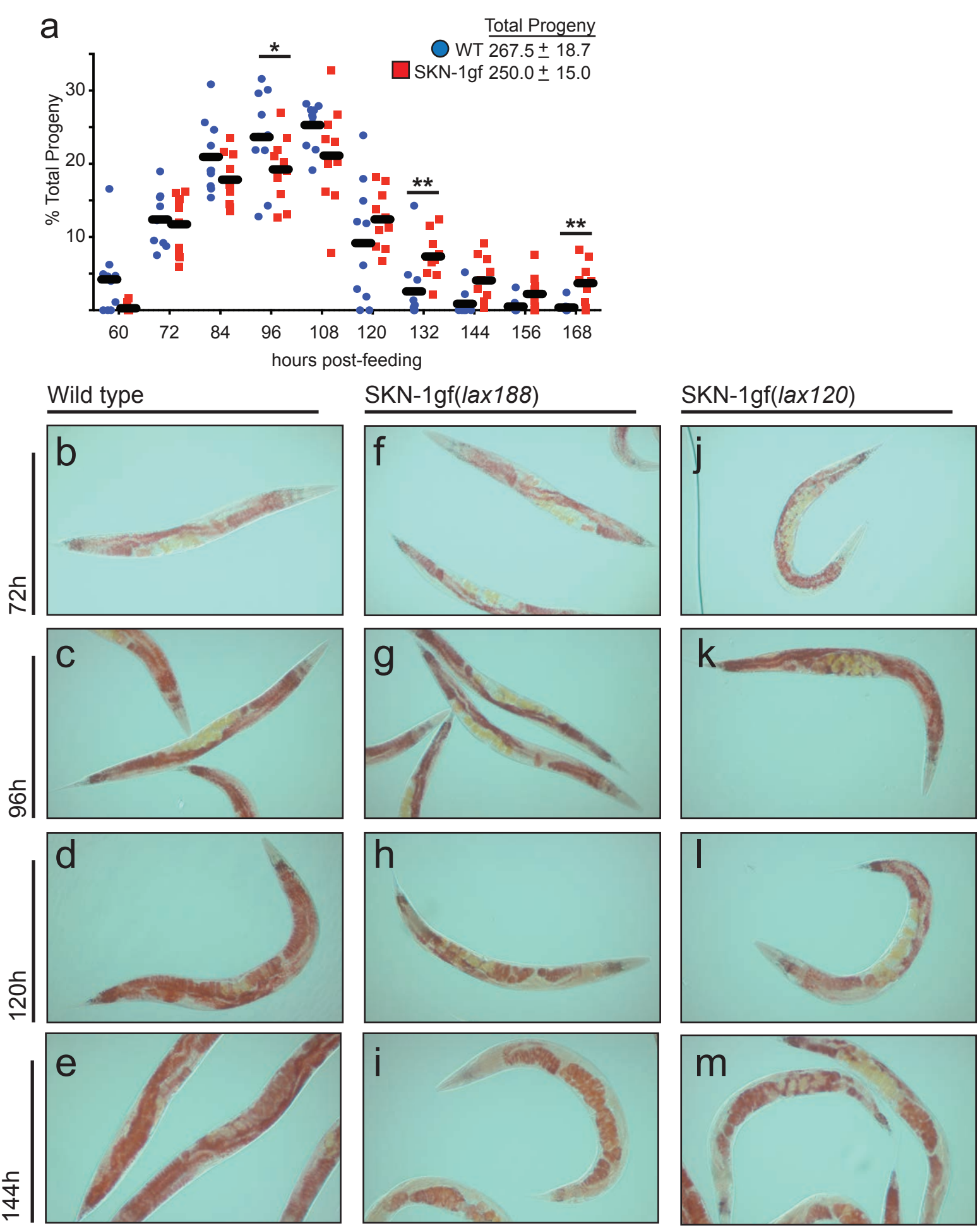

Lynn et al.
Figure S1

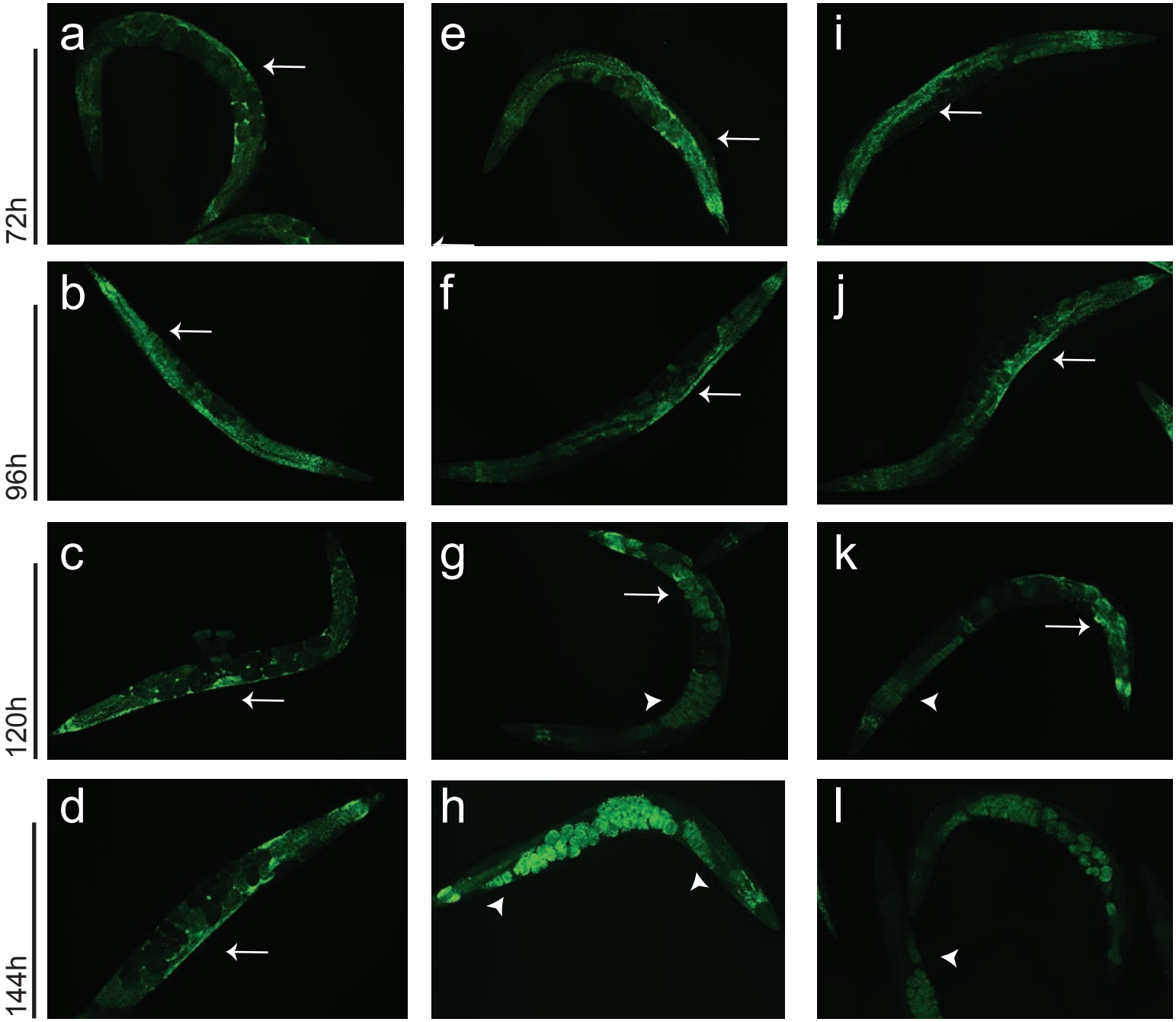

Lynn et al.
Figure S2

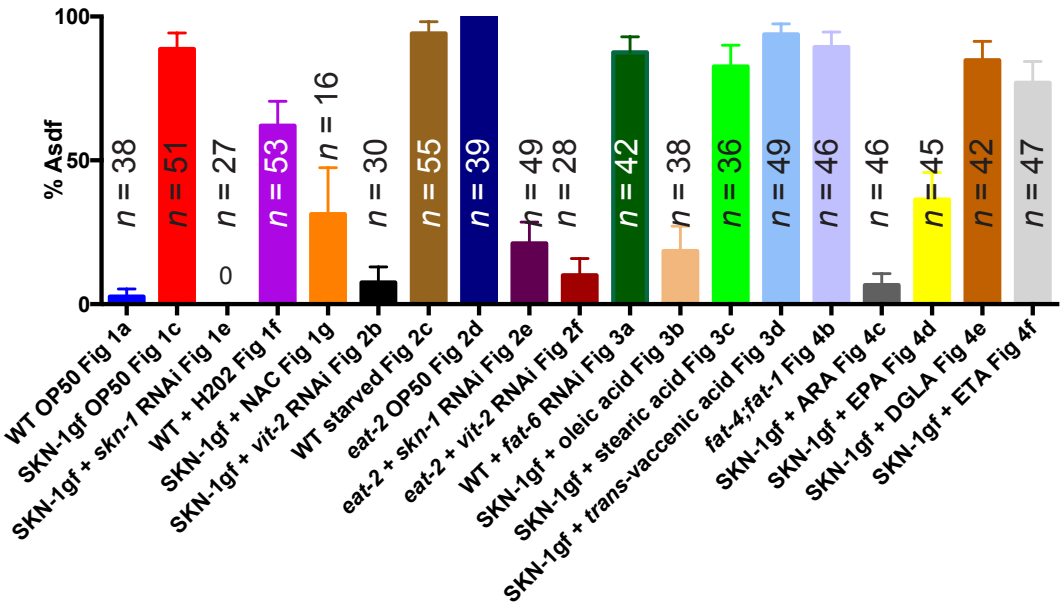

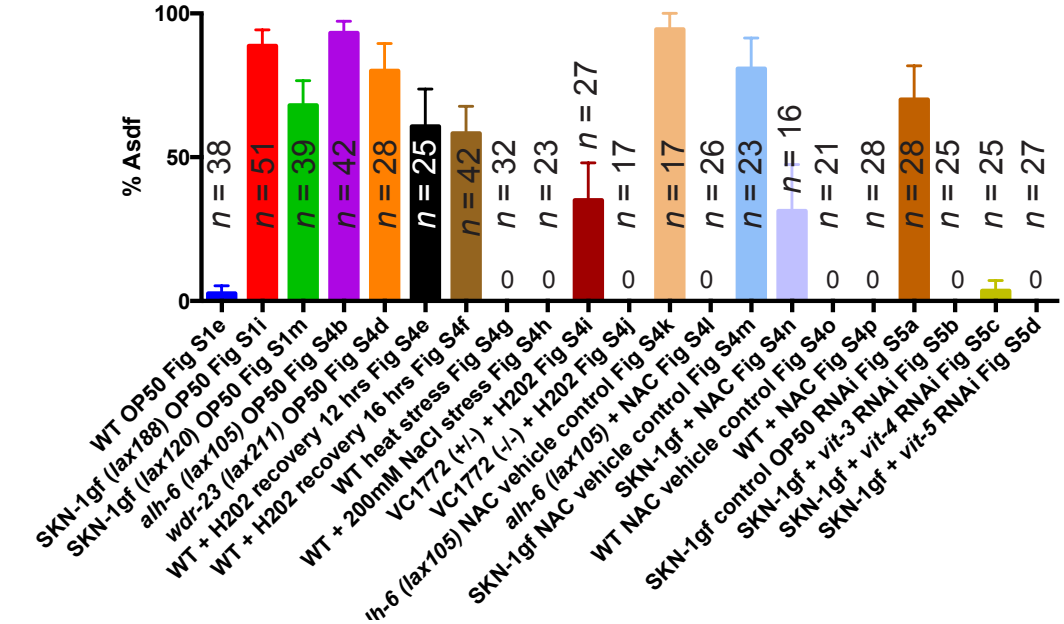

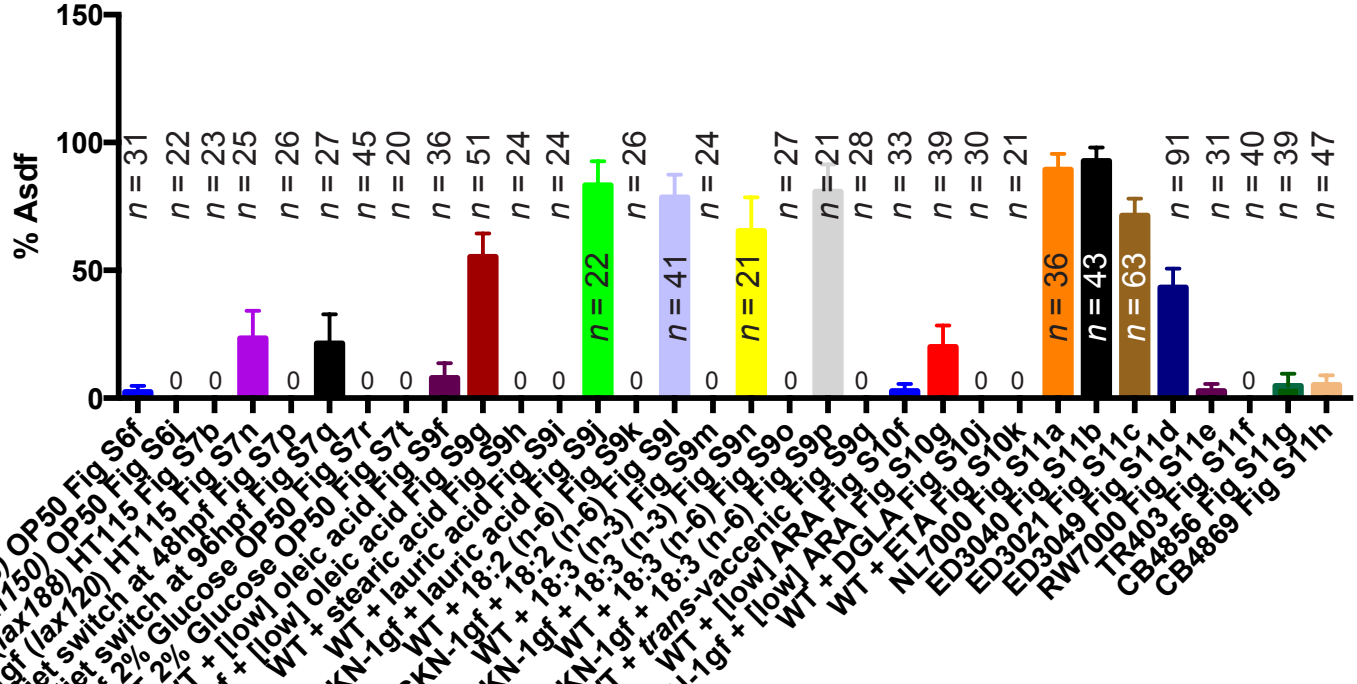

Lynn et al.
Figure S3

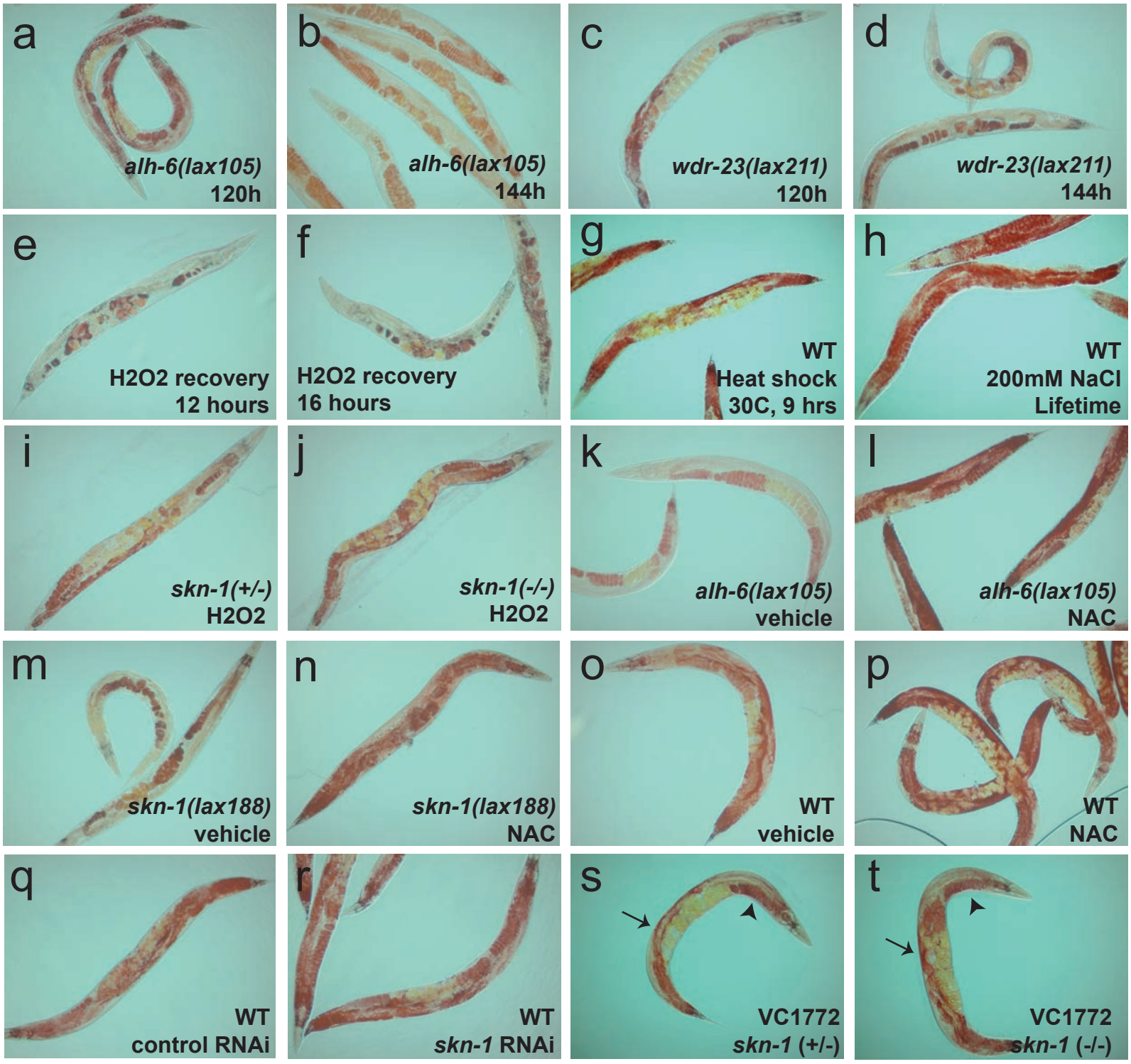

Lynn et al.
Figure S4

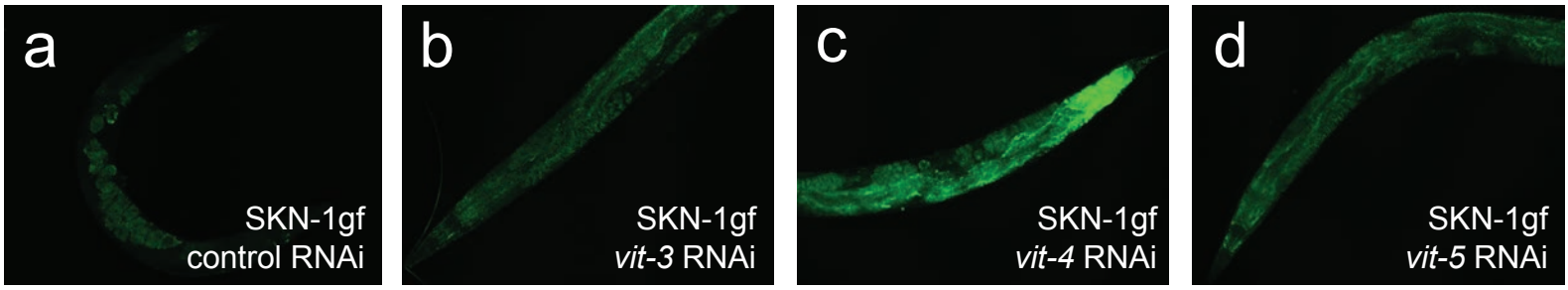

Lynn et al.
Figure S5

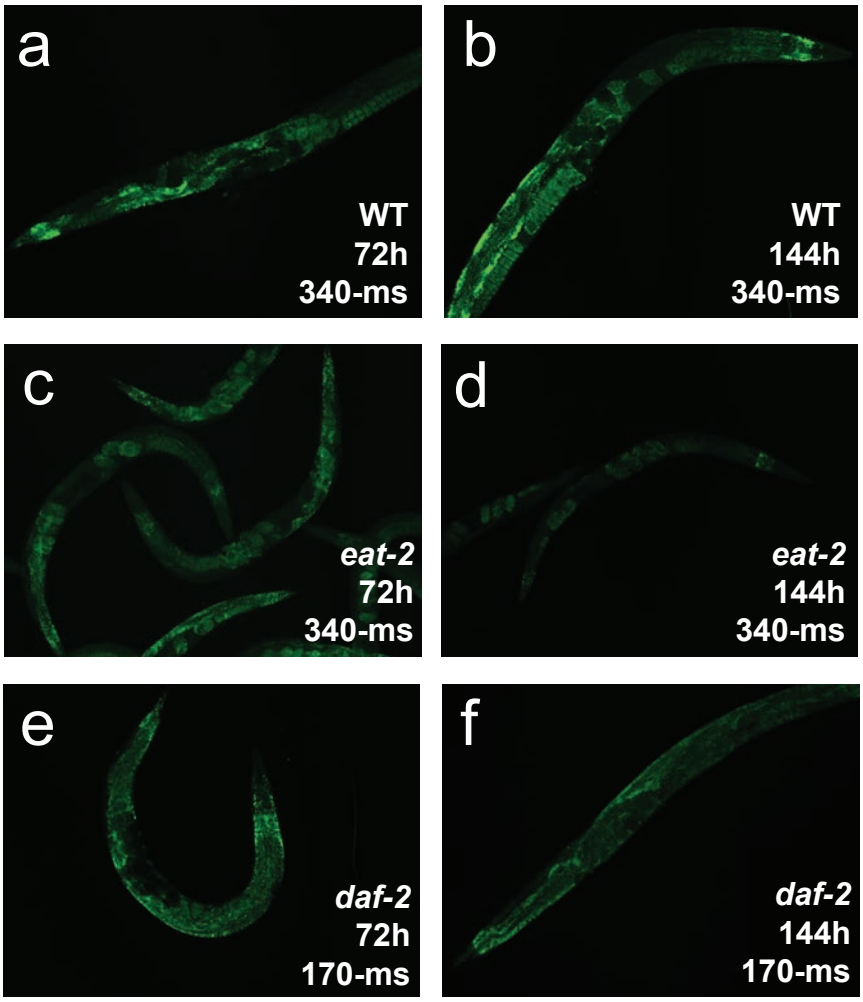

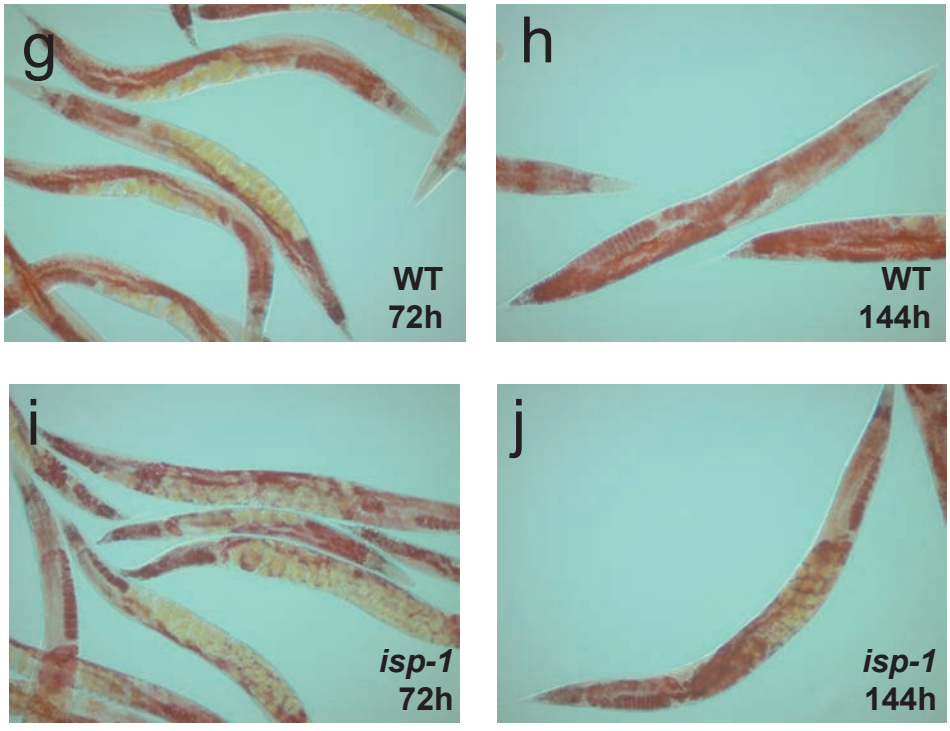

Lynn et al.
Figure S6

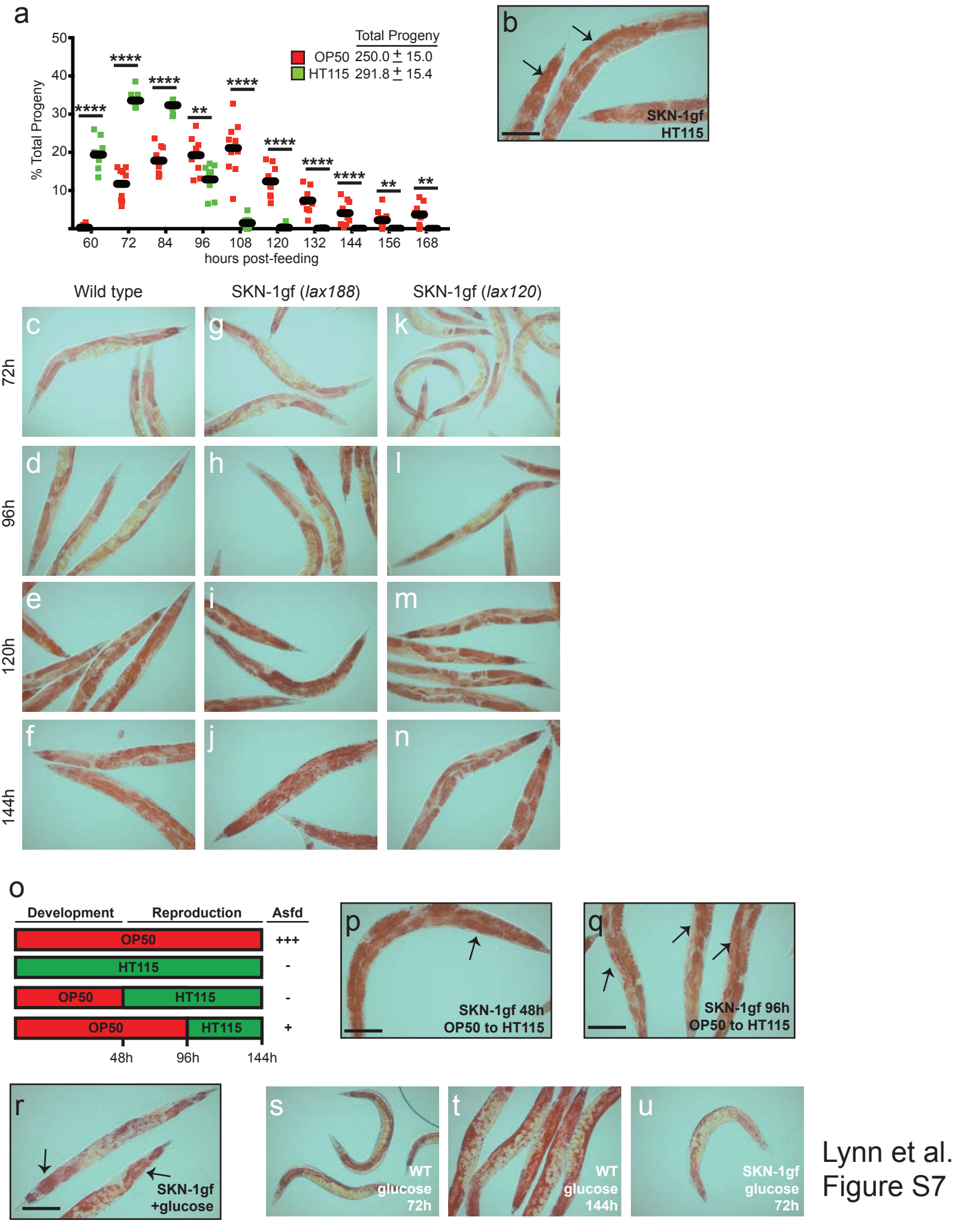

Lynn et al.
Figure S7

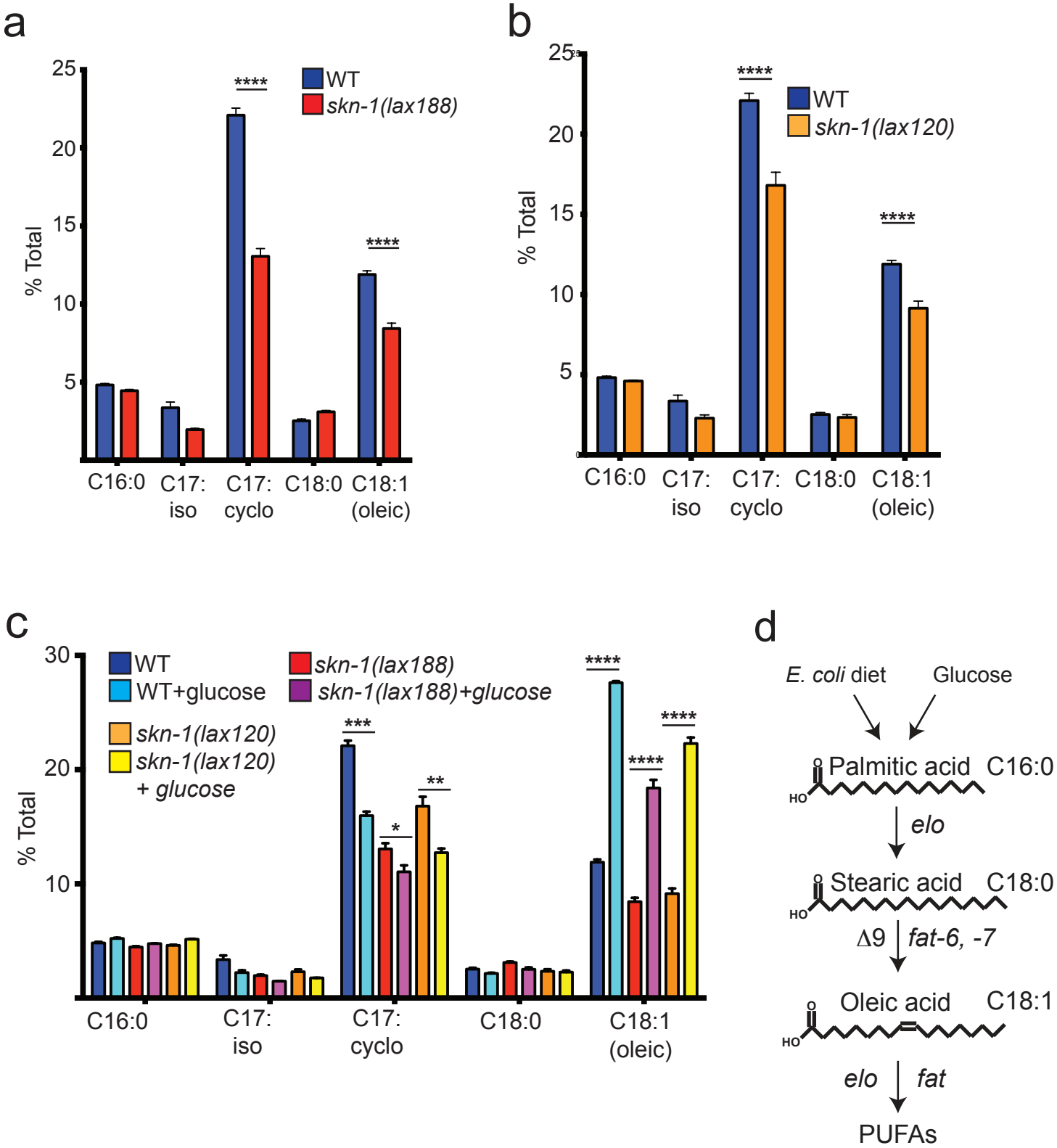

Lynn et al.
Figure S8

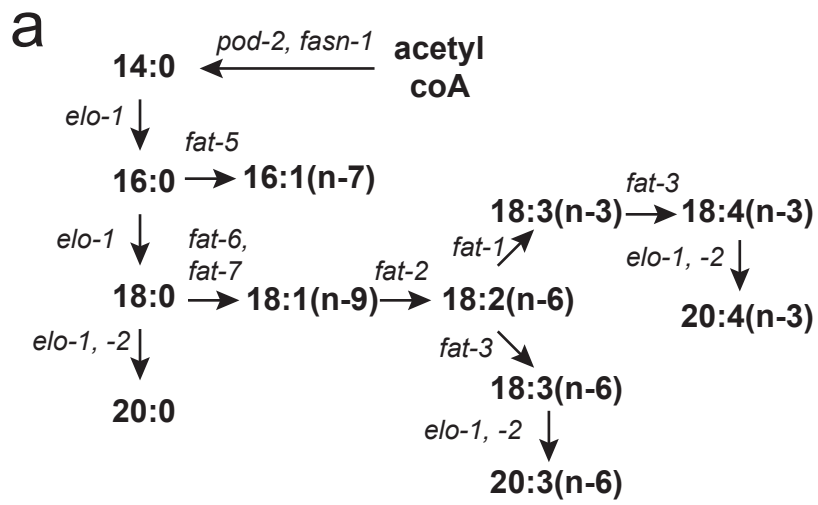

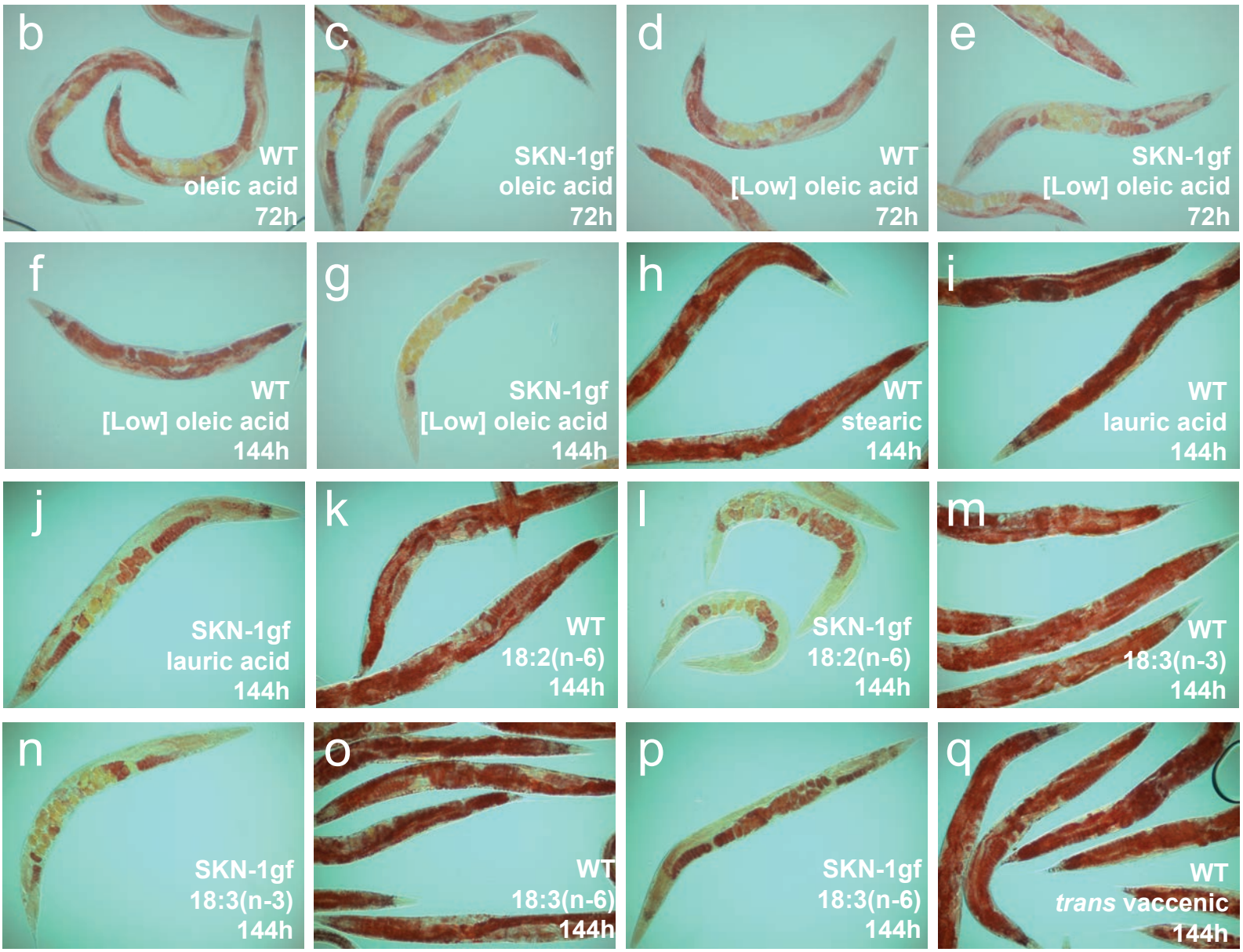

Lynn et al.
Figure S9

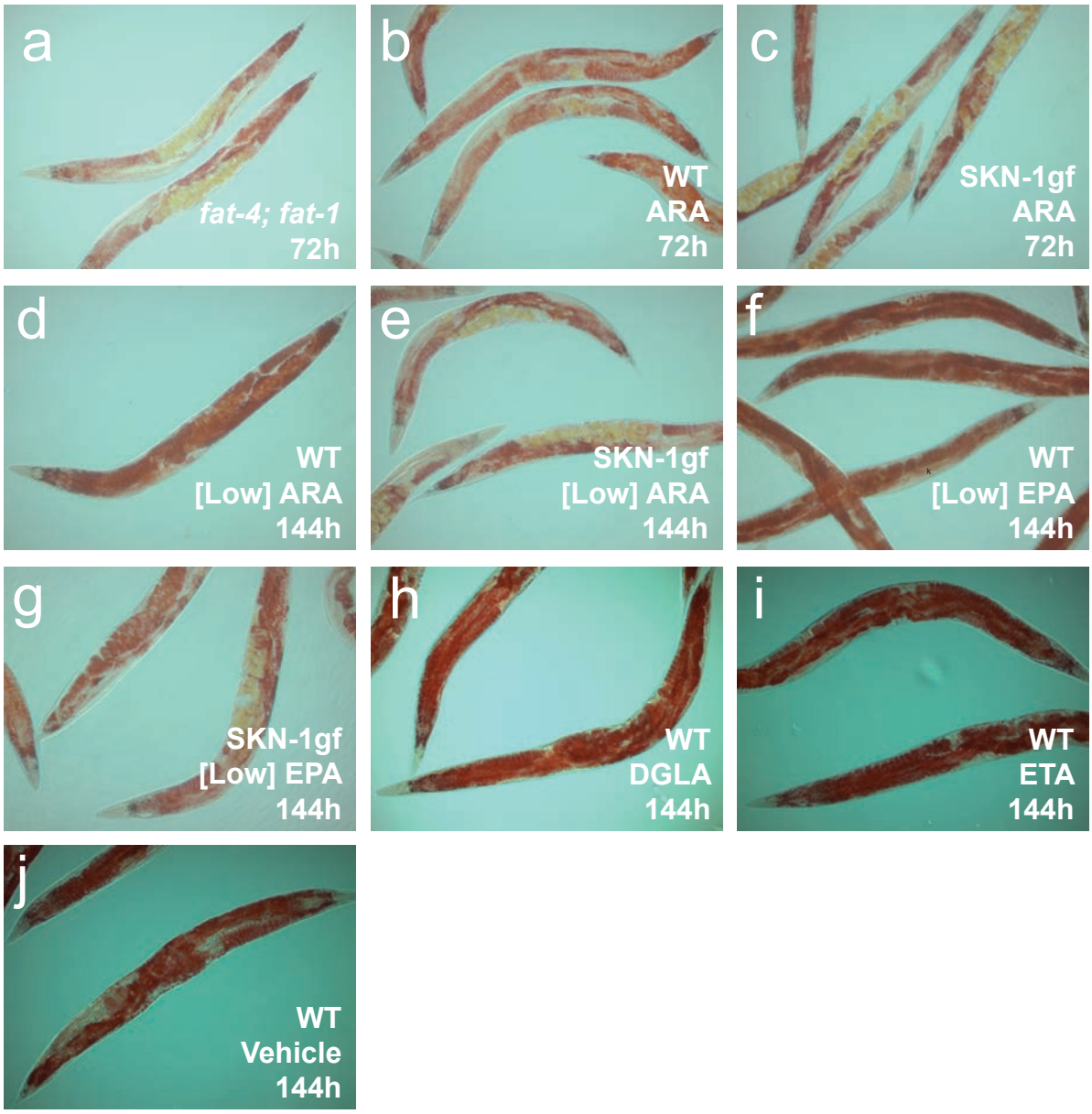

Lynn et al.
Figure S10

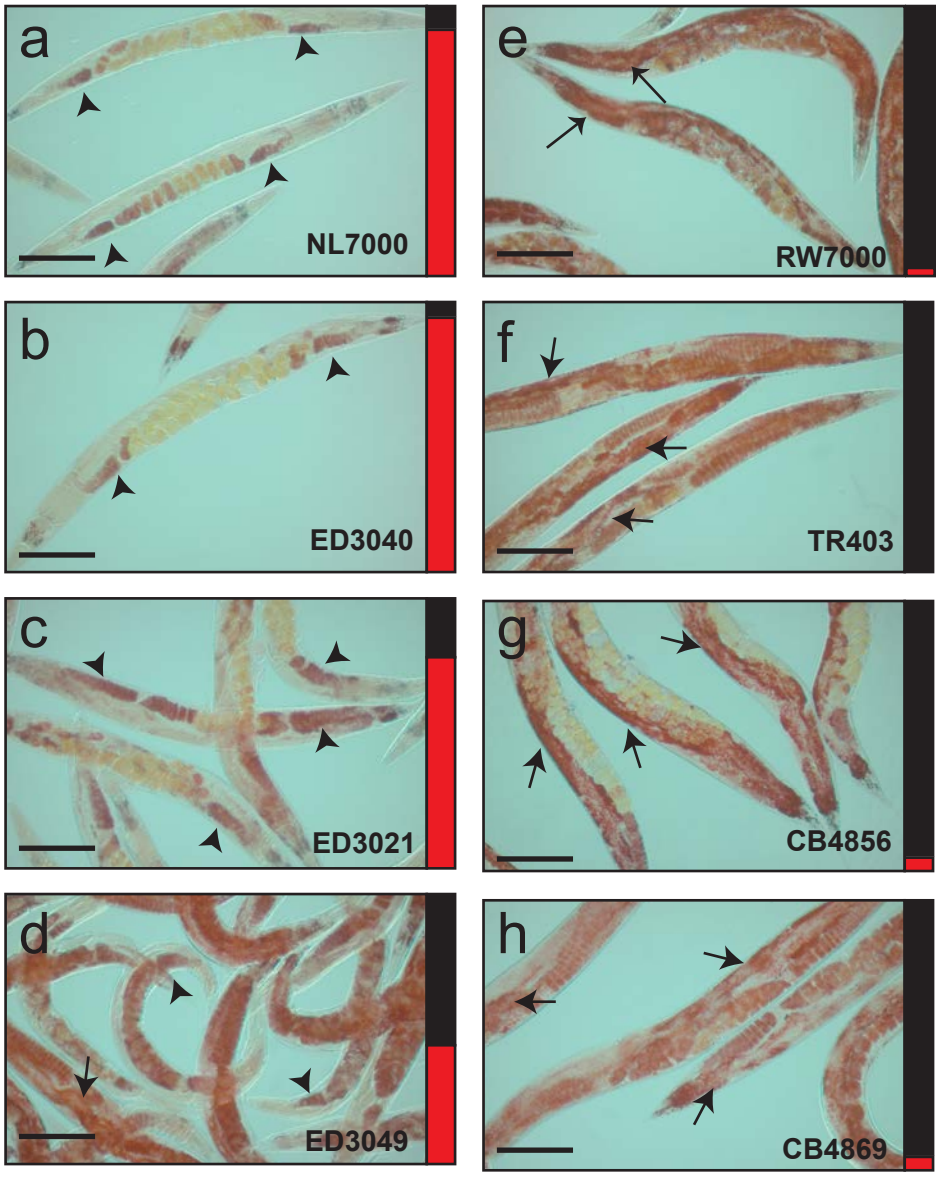

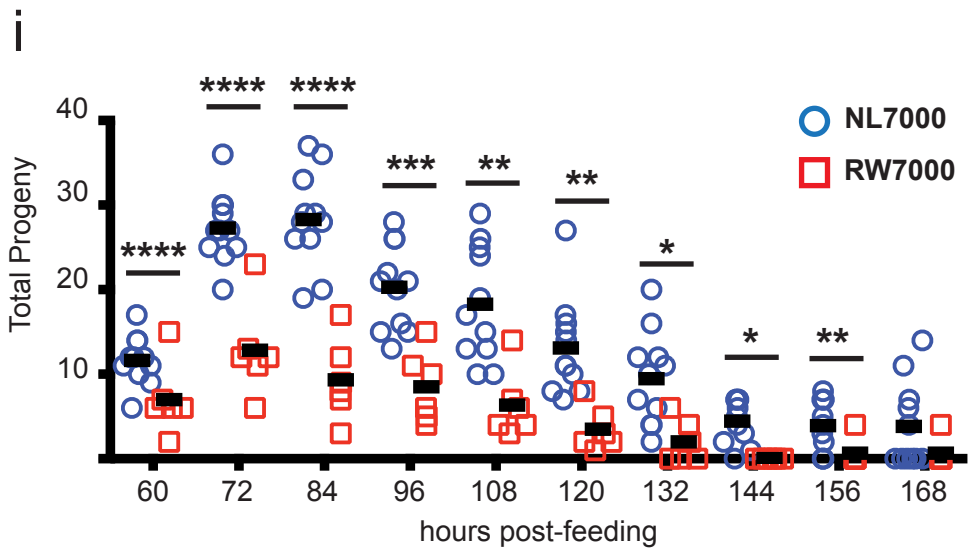

Lynn et al.
Figure S11

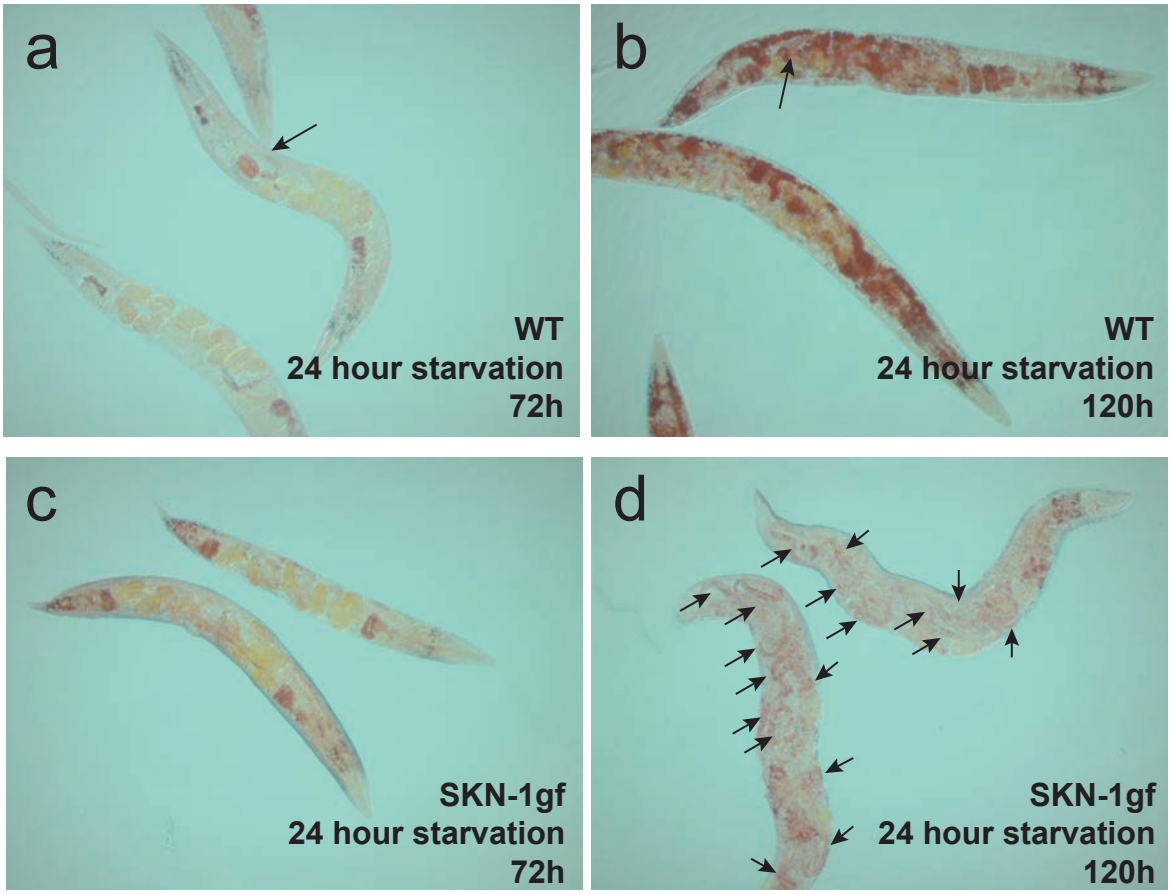

Lynn et al.
Figure S12

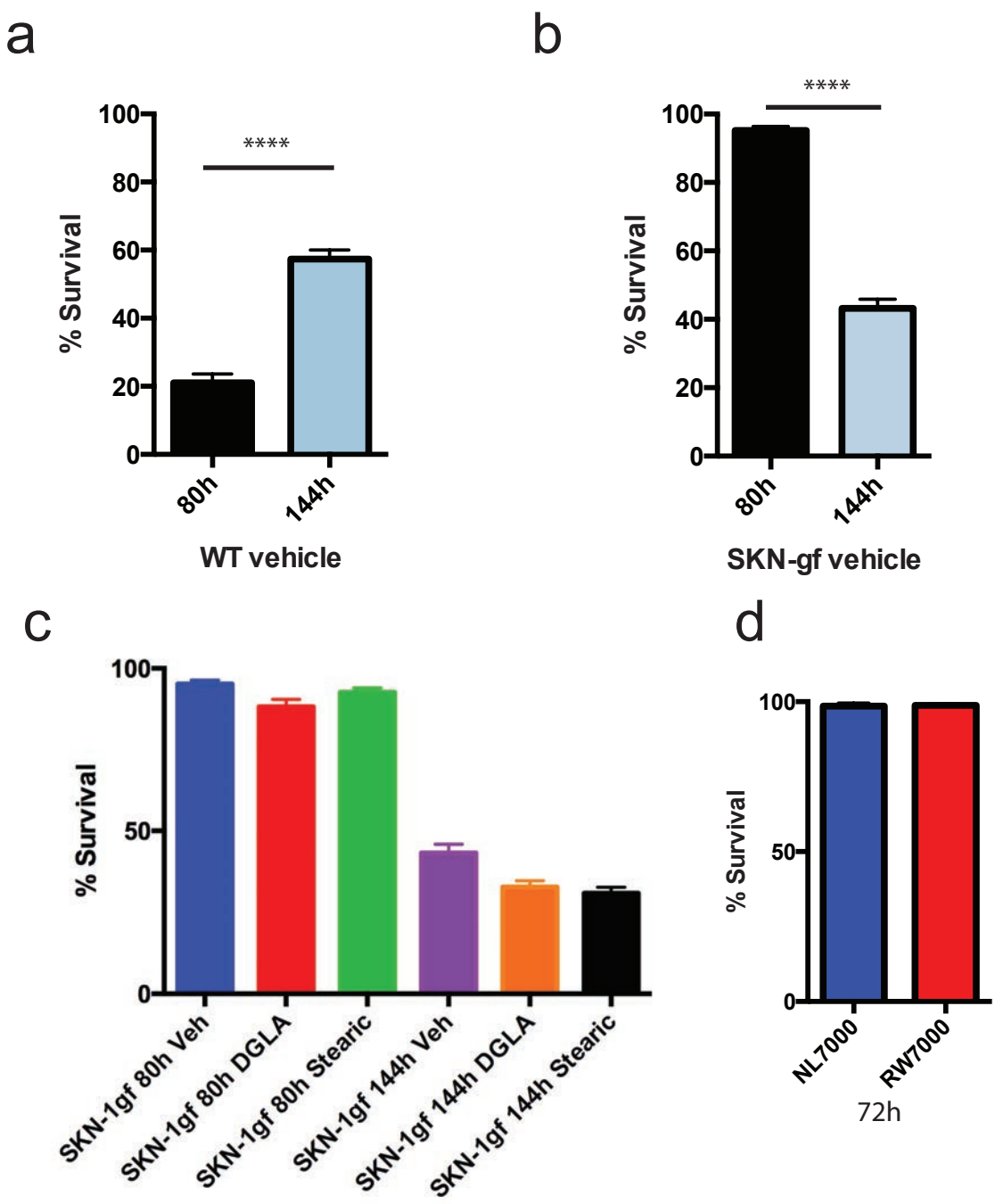

Lynn et al.
Figure S13